

Direct synthesis of a 9×10 member ring zeolite (Al-ITQ-13): A highly shape-selective catalyst for catalytic cracking

R. Castañeda, A. Corma*, V. Fornés, J. Martínez-Triguero, S. Valencia

Instituto de Tecnología Química (UPV-CSIC), Universidad Politécnica de Valencia, Avenida de los Naranjos s/n. 46022 Valencia, Spain

Received 6 October 2005; revised 25 November 2005; accepted 28 November 2005

Available online 9 January 2006

Abstract

A synthesis route for preparing ITQ-13, a tridirectional medium-pore zeolite containing 9- and 10-member ring pores, has been found that allows the introduction of framework Al by direct synthesis. It has been shown that ITQ-13 can also be prepared in a fluoride-free media. The directly synthesized Al containing ITQ-13 sample presents acid sites as strong or even stronger than ZSM-5. The strong electric field gradient in ITQ-13 and the smaller pore dimensions are responsible for the strong acidity and shape selectivity that increases the production of propylene during the cracking of vacuum gasoil compared with ZSM-5.

© 2005 Elsevier Inc. All rights reserved.

Keywords: ITQ-13; Zeolite; Catalytic properties; 10×9 member ring pore zeolite; Propylene production in catalytic cracking; Zeolite-cracking additive

1. Introduction

There is a continuous effort in industry and academia to obtain new zeolite structures, as well as to modify the characteristics of the existing ones [1–3]. Various series of new structures with extra large, large, medium, and small pore sizes have been reported [4–18].

Medium pore size zeolites—those formed by 10-member ring (MR) channels, such as ferrierite [19], ZSM-22 [20], Theta-1 [21], SSZ-35 [22], and especially ZSM-5 [23]—have been successful shape-selective catalysts [24]. More specifically, ZSM-5 has strongly enhanced the possibilities of FCC units through shape-selective cracking of *n*-olefins to increase the formation of propylene [25]. Cracking of model hydrocarbons using a large number of zeolites with different pore dimensions and topologies led to predictions that zeolites with a bidirectional or tridirectional pore system formed by 9 or 9×10 MR should be very adequate FCC additives for boosting propylene [26,27]. Recently, a new zeolite (ITQ-13) was synthesized [28] that presents a tridirectional set of channels in

which one of them has 9 MR (4.0×4.9 Å) openings and the other two channels are straight (4.7×5.1 Å) and sinusoidal 10 MR (4.8×5.7 Å) [29].

Zeolite ITQ-13 is described as a material prepared in fluoride media with hexamethonium as an organic structure-directing agent (OSDA) that is able to incorporate boron in the framework by isomorphic substitution of silicon during synthesis [28]. By means of a postsynthesis treatment, it was possible to exchange aluminium with boron, giving Al-ITQ-13, a material of sufficient acidity for catalytic activity [30]. Unfortunately, in the previously reported synthesis [28] it was found extremely difficult to directly synthesize the aluminosilicate form of ITQ-13 with significant levels of aluminium.

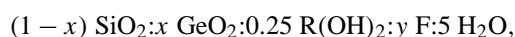
In this paper we describe a new synthesis route for ITQ-13 that allows us to readily incorporate framework Al during the synthesis, resulting in very thermally and hydrothermally stable samples. We also show that this synthesis route makes it possible to synthesize ITQ-13 in a fluoride-free media. Acid samples showed cracking activity close to that of ZSM-5, but with a much higher propylene-to-propane ratio in the gases when used as a catalyst additive for cracking vacuum gasoil.

* Corresponding author. Fax: +34 96 3877809.
E-mail address: acorma@itq.upv.es (A. Corma).

2. Experimental

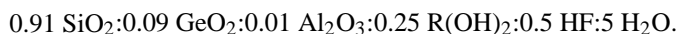
2.1. Materials

ITQ-13 zeolites were synthesized from synthesis mixtures prepared by dissolving the appropriate amount of GeO₂ (99.998%, Aldrich) in an aqueous solution of hexamethonium dihydroxide (R(OH)₂). Then tetraethylorthosilicate (TEOS) (98%, Merck) was added, and the resulting solution was mechanically stirred until the hydrolysis of TEOS was completed and any ethanol generated was totally evaporated. Finally, for synthesis in fluoride media, the required amount of hydrofluoric acid (48% aqueous solution, Aldrich) or ammonium fluoride (98%, Aldrich) was added. The final synthesis gels had the following molar composition:



where x was varied between 0 and 0.17 and y was varied between 0 and 0.5. In some experiments, 10 wt% ITQ-13 seeds (with respect to the inorganic oxides) were added to promote crystallization. The gels were autoclaved at 448 K for the required time under continuous stirring at 60 rpm. Then the solids were recovered by filtration, washed with distilled water, and dried at 373 K overnight.

The Al-ITQ-13 material was synthesized following the same procedure, but adding the appropriate amount of Al isopropoxide (98%, Aldrich) and performing the crystallization at 408 K instead of 448 K. The final synthesis gel had the following molar composition:



The occluded hexamethonium cations were removed by heating in air from room temperature to 623 K at a rate of 1 K min⁻¹, and maintaining this temperature for 3 h. Then, the temperature was raised at a rate of 1 K min⁻¹ up to 853 K. The product was kept at this temperature for 3 h to burn off the remaining organic.

ZSM-5 zeolite with a Si/Al ratio of 40 was obtained from Zeolyst (CBV8020). ZSM-5 (Si/Al = 15) with crystal sizes of 0.2, 0.5, and 1 μm were obtained from Tricat Zeolites GmbH (codes TZP-322, TZP-302A, and TZP-302H, respectively).

2.2. Sample characterization

Crystallinity measurement and phase identification of the materials was carried out by powder X-ray diffraction (XRD) with a Phillips X'Pert MPD diffractometer equipped with a PW3050 goniometer (Cu-K_α radiation, graphite monochromator) provided with a variable divergence slit. Infrared (IR) experiments were performed in a Nicolet 710 Fourier transform IR (FTIR) spectrometer using vacuum cells. After the 10-mg cm⁻² wafers were degassed overnight under vacuum (10⁻³ Pa) at 673 K, the base spectra were recorded at room temperature. For acidity measurements, pyridine (6 × 10² Pa) was admitted. After equilibration, the samples were outgassed for 1 h at increasing temperatures (423/523/623 K). After each desorption step, the spectrum was recorded at room temperature

and the background subtracted. Determination of the concentration of Brönsted and Lewis acid sites was derived from the area of the IR bands at ca. 1550 (IA_B) and 1450 cm⁻¹ (IA_L), respectively, by applying the following equations from Emeis [31]:

$$C_B = 1.88 \cdot \text{IA}_B \cdot R^2 / W$$

and

$$C_L = 1.42 \cdot \text{IA}_L \cdot R^2 / W,$$

where B represents Brönsted acid center, L represents Lewis acid center, C is concentration (mmol/g catalyst), IA is integrated absorbance, R is the radius of the catalyst disk (cm), and W is the weight of the disk (mg).

Solid-state ²⁷Al MAS NMR spectra were recorded at 104.2 MHz with a spinning rate of 7 kHz and at a 9° pulse length of 0.5 μs and a repetition time of 0.5 s, and chemical shifts were reported relative to Al(H₂O)₆³⁺. Chemical composition was determined by atomic absorption in a Varian SpectrAA-10. Micropore volume was measured by nitrogen adsorption/desorption isotherms in a Micromeritics ASAP 2000.

2.3. Reaction procedure

Cracking experiments were performed in a microactivity test unit as described previously [32]. The cracking of *n*-decane was done at 773 K and 60 s time on stream (TOS). Then 0.5 g of zeolite was pelletized, crushed, and sieved, and the 0.59–0.84 mm fraction was taken and diluted in 2.5 g of inert silica. Conversion was defined as the sum of the yields of all products different from *n*-decane, including coke. For each catalyst, five experiments were performed, maintaining the amount of catalyst (cat) constant and equal to 0.5 g and varying the *n*-decane amount (oil) fed between 0.77 and 1.54 g.

The cracking of vacuum gasoil was performed at 793 K and 30 s TOS as described previously [32]. ZSM-5 and Al-ITQ-13 samples were tested as additives of USY zeolite (CBV760 from Zeolyst; unit cell, 2.426 nm). The percentage of additive used corresponds to the weight of zeolitic additive per 100 g of USY zeolite.

3. Results and discussion

The introduction of Ge in the gel allows the synthesis of ITQ-13 with high crystallinity while GeO₂ is not detected by XRD in both the as-synthesized and calcined samples (Fig. 1). As occurs with other zeolites containing double four-member rings as secondary building units [13,33,34], the introduction of Ge into the synthesis media increases the rate of nucleation and consequently diminishes the synthesis time (Fig. 2). It is remarkable that the germanium silicates obtained with Si/Ge ratios as low as 5 are stable after calcination at 853 K in the presence of moisture. This is evidenced by the corresponding XRD measurements, as well as by surface area and micropore volume determinations (Table 1). It appears that then the structure of Ge-ITQ-13, a zeolite with a relatively high framework

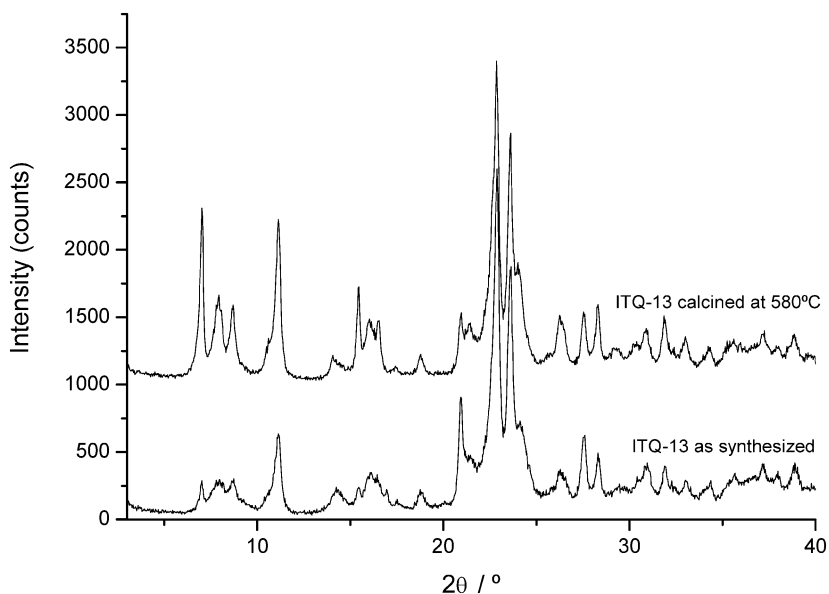


Fig. 1. XRD patterns of as-synthesized (bottom) and calcined (top) ITQ-13 zeolite with Si/Ge = 10.

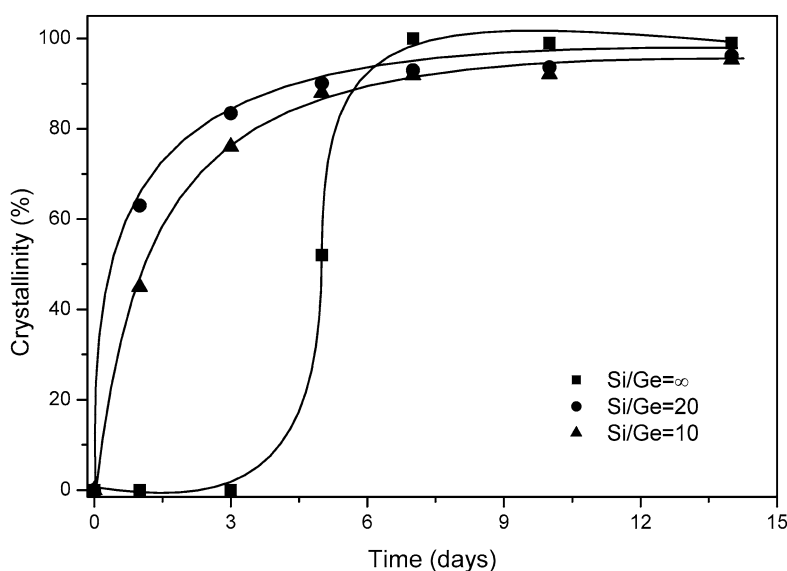


Fig. 2. Crystallization curves of ITQ-13 zeolites with different Si/Ge ratio prepared in fluoride media.

Table 1
Textural properties of Ge-ITQ-13 samples prepared in fluoride media and calcined at 853 K in the presence of moisture

(Si/Ge) _{gel}	(Si/Ge) _{analysis}	S _{BET} (m ² g ⁻¹)	V _{micro} (cm ³ g ⁻¹)
∞	∞	383	0.169
25	20.9	398	0.165
20	16.7	360	0.148
10	9.2	410	0.154
5	6.0	383	0.151

density, is more stable than other large-pore germanium silicates that require Si/Ge ratios >10 to maintain the crystalline structure on calcination in the presence of moisture [9,33,35].

Chemical analyses of the Ge-ITQ-13 zeolites prepared in fluoride media show good agreement between the Si/Ge ra-

tio in the solids and in the corresponding gels (see Table 1), suggesting that all of the Ge was successfully incorporated in framework positions.

3.1. Effect of Ge and F⁻ concentrations

The results given in Table 2 show that during the synthesis, two phases—a layered material (L) and EU-1 zeolite—are competing with ITQ-13. As the table indicates, ITQ-13 formation is favored over EU-1 or the layered phase when increasing the concentration of F⁻, probably due to the stabilization of D4R and [4¹5²6²] cages by F⁻ ions [36]. When the equivalent of one F⁻ ion per D4R (stoichiometric amount of fluoride) is introduced in the synthesis gel, EU-1 strongly competes with ITQ-13. But when at the same F⁻ concentration the germanium content in the synthesis gel is increased, ITQ-13 is the

Table 2
Results of the synthesis of ITQ-13 carried out in different conditions

Experiment	Si/Ge	F/ (Si + Ge) ^a	Seeds	Time (days)	XRD phases ^b
1	10	0	no	7	L
				18	L + ITQ-13 + EU-1
				25	ITQ-13
2	10	0	yes	7	ITQ-13
				10	ITQ-13
3	10	0.07	no	7	L + ITQ-13
				10	ITQ-13
4	10	0.07	yes	7	ITQ-13
				10	ITQ-13
5	10	0.5	no	5	ITQ-13
				10	ITQ-13
6	20	0	no	7	L
				18	L + ITQ-13
				25	ITQ-13
7	20	0	yes	4	L + ITQ-13
				17	ITQ-13
8	20	0.07	no	7	L + EU-1 + ITQ-13
				18	ITQ-13 + EU-1
9	20	0.07	yes	7	L + ITQ-13
				14	ITQ-13
10	20	0.5	no	5	ITQ-13
				10	ITQ-13
11	∞	0.5	no	5	ITQ-13 + am
				7	ITQ-13

^a The ratio F/(Si + Ge) = 0.07 corresponds to the “stoichiometric amount of fluoride.” All the syntheses were performed at 175 °C with H₂O/(Si + Ge) = 5 and R(OH)₂/(Si + Ge) = 0.25.

^b L: layered phase; am: amorphous material.

only crystalline phase formed, clearly demonstrating the directing effect of Ge toward structures containing double four rings (D4R) as secondary building units. If seeds of ITQ-13 are introduced in the Ge-assisted synthesis to accelerate the crystallization rate, then pure ITQ-13 can be produced with a stoichiometric amount of fluoride in almost the same time as required with high concentrations of F⁻ and without germanium. The directing effect of Ge is so strong in this case that with Si/Ge ratios of 20 in the gel, it is possible to synthesize ITQ-13 in a fluoride-free OH⁻ media (see Table 2, experiments 1, 2, 6, and 7).

3.2. Framework insertion of Al

With the previously reported synthesis of ITQ-13 [28], introducing framework Al during the synthesis was difficult. Al in the synthesis gel diminishes the crystallization rate of ITQ-13, while favoring the formation of EU-1. On the other hand, boron could be inserted in the ITQ-13 structure during synthesis, although in relatively small amounts, resulting in framework Si/B ratios >50. Most likely the shorter T–O–T angles in the boron sample facilitate its introduction with respect to the EU-1 structure. Nevertheless, ion exchange of aluminium by boron in a postsynthesis treatment [37] results in aluminosilicates exhibiting acidity associated with the presence of tetrahedrally coordinated Al.

The results from carrying out the Al exchange in a boron ITQ-13 with Si/B = 60 (sample SiAl(B)-ITQ-13) indicate that

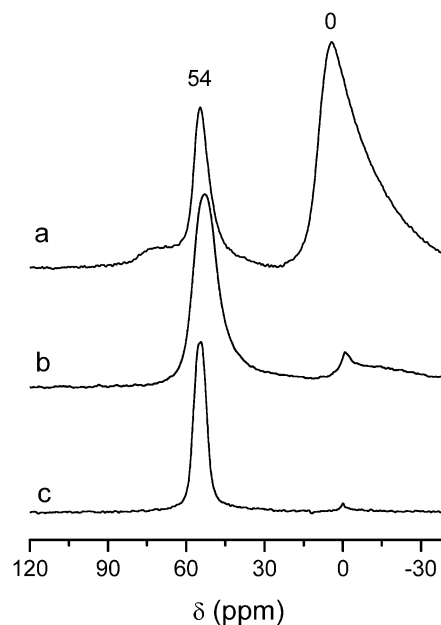


Fig. 3. ²⁷Al MAS NMR spectra of Al-ITQ-13 zeolites: (a) SiAl(B)-ITQ-13 sample, (b) SiGeAl-ITQ-13 sample, and (c) ZSM-5 sample.

Table 3

Acidic properties and crystal size of different ITQ-13 samples and ZSM-5 determined by pyridine desorption from the IR spectra

Sample	Crystal size (μm)	Brönsted ^a (μmol g ⁻¹)			Lewis ^a (μmol g ⁻¹)		
		423 K	523 K	623 K	423 K	523 K	623 K
ZSM-5	0.5–1	113	92	44	23	17	13
SiAl(B)-ITQ-13 ^b	0.5–1.5	45	36	13	103	100	85
SiGeAl-ITQ-13 ^c	0.5–3	63	55	28	48	32	27

^a Extinction coefficients from [31].

^b Si/Al = 80, obtained by a post-synthesis ion exchange of Al by B from a starting ITQ-13 sample of Si/B = 60.

^c Si/Ge = 10; (Si + Ge)/Al = 50.

although all of the boron was removed from the zeolite during the treatment, only a fraction was exchanged by aluminium, resulting in an ITQ-13 sample with a Si/Al molar ratio of 80. It becomes then evident that the total number of acid sites in the Al-ITQ-13 prepared in two steps was lower than the potential acidity given by the original T^{IV}/T^{III} ratio.

Interestingly, when Ge is present in the synthesis gel, the aluminium containing ITQ-13 can be easily synthesized with (Si + Ge)/Al ratios as low as 30. The ²⁷Al MAS NMR spectrum shows that Al is tetrahedrally coordinated (spectrum not shown). After calcination, a small amount of octahedral Al is evidenced in the spectrum (Fig. 3b), whereas in sample SiAl(B)-ITQ-13, a large amount of octahedral Al was clearly visible at 0 ppm (Fig. 3a). This indicates that even though the framework (Si + Ge)/Al ratio of the as synthesized SiGeAl-ITQ-13 sample was 50, part of the framework Al was removed during calcination, being the framework (Si + Ge)/Al ratio of the calcined zeolite >50. All of these findings should reflect on the acidity of the samples. As shown in Table 3, the directly synthesized Al sample has higher Brönsted acidity as measured by pyridine adsorption–desorption. More specifically, the Brön-

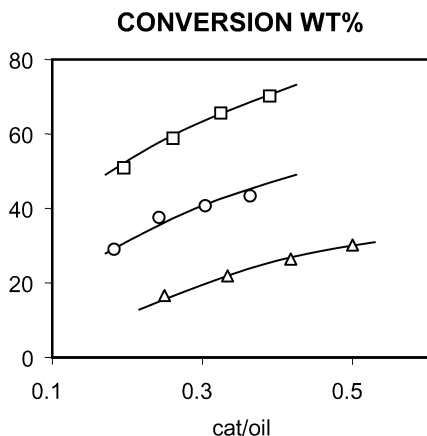


Fig. 4. Total conversion in the cracking of *n*-decane at 773 K and 60 s time on stream over (□) ZSM-5, (○) SiGeAl-ITQ-13 and (△) SiAl(B)-ITQ-13.

Table 4

First order kinetic rate constant and turnover frequency in the *n*-decane cracking at 773 K and 60 s time on stream

	K ($\text{g}_{\text{oil}} \text{g}_{\text{cat}}^{-1} \text{s}^{-1}$)	TOF $\times 10^3$ (K/PyB 423 K)
ZSM-5	0.088	0.78
SiAl(B)-ITQ-13	0.013	0.29
SiGeAl-ITQ-13	0.040	0.63

sted acidity measured by the pyridine remaining adsorbed at 423 K is ~ 1.4 times larger than for SiAl(B)-ITQ-13, whereas from the nominal composition it should be ~ 1.6 times larger, demonstrating the effect of dealumination during the calcination procedure. Thus, as would be expected, more pyridine is coordinated to Lewis acid sites for SiAl(B)-ITQ-13.

3.3. Catalytic results

The differences in acidity demonstrated by the Al-ITQ-13 samples (see Table 3) should have an important impact on catalytic activity. In an attempt to confirm this statement, we first chose as reactant a linear alkane (*n*-decane) that can penetrate in both 9 and 10 MR, and the cracking activity of a ZSM-5 has been compared with two Al-ITQ-13 samples: one (SiAl(B)-ITQ-13) prepared in the boron form and then exchanged with aluminium and the other (SiGeAl-ITQ-13) directly synthesized with Al in the framework. *n*-Decane conversion at different contact times is plotted in Fig. 4, and the first-order kinetic rate constants are given in Table 4. The results show that ZSM-5 is the most active, followed by the directly synthesized Al-ITQ-13. On the other hand, evaluating the acidity of the samples, as measured by pyridine adsorption–desorption (see Table 3), demonstrates that the total Brønsted acidity is higher in ZSM-5, corresponding to its higher Al content (Si/Al = 40). But even if the potential acidity is taken into account (i.e., $T^{\text{III}} / (T^{\text{III}} + T^{\text{IV}})$), ZSM-5 still has more Brønsted acid sites than the directly synthesized SiGeAl-ITQ-13. This could be explained by assuming that pyridine is diffusion-controlled through the 9 MR pores and thus may not see all of the potential acid sites in ITQ-13. To test this hypothesis, we measured IR spectra of the

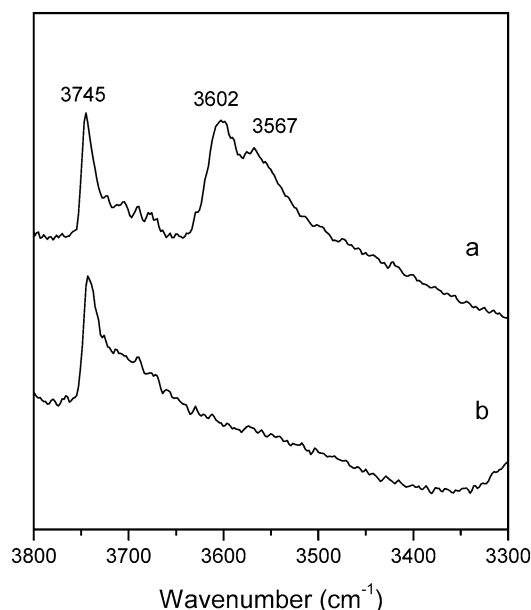


Fig. 5. IR spectra of SiGeAl-ITQ-13 sample in the OH region (a) original spectrum (673 K and vacuum) and (b) after pyridine adsorption and desorption at 423 K.

Table 5

Vacuum gasoil properties

Density (333 K) (g cc^{-1})	0.916
Aniline point (K)	349
Sulfur (wt%)	2.7
Nitrogen (wt%)	0.15
Carbon Conradson (%)	0.09
Na (ppm)	<0.05
Cu (ppm)	30
Fe (ppm)	0.5
Ni (ppb)	30
V (ppb)	<25
ASTM D-1160 (K)	
10%	673
30%	684
50%	698
70%	722
90%	762

SiGeAl-ITQ-13 sample in the OH region before and after adsorption of pyridine followed by desorption in vacuum at 423 K. The results, shown in Fig. 5, appear to show that all of the OH groups at 3602 and 3567 cm^{-1} interacted with pyridine, indicating that, as far as the spectra show, pyridine can reach all potential acid sites. Therefore, differences in pyridine diffusion cannot explain the lower number of acid sites observed in the ITQ-13 samples.

A second hypothesis to explain the relative acidity could be lower stability (higher dealumination) of SiGeAl-ITQ-13 with respect to ZSM-5 due to the presence of Ge in the former sample. If this were the case, then a greater amount of extra-framework Al would be formed in SiGeAl-ITQ-13. For the calcined SiGeAl-ITQ-13 zeolite, ^{27}Al MAS NMR revealed two peaks at ~ 54 and 0 ppm (Fig. 3b), the second peak associated with extra-framework Al (EFAL) [38]. The NMR spectra

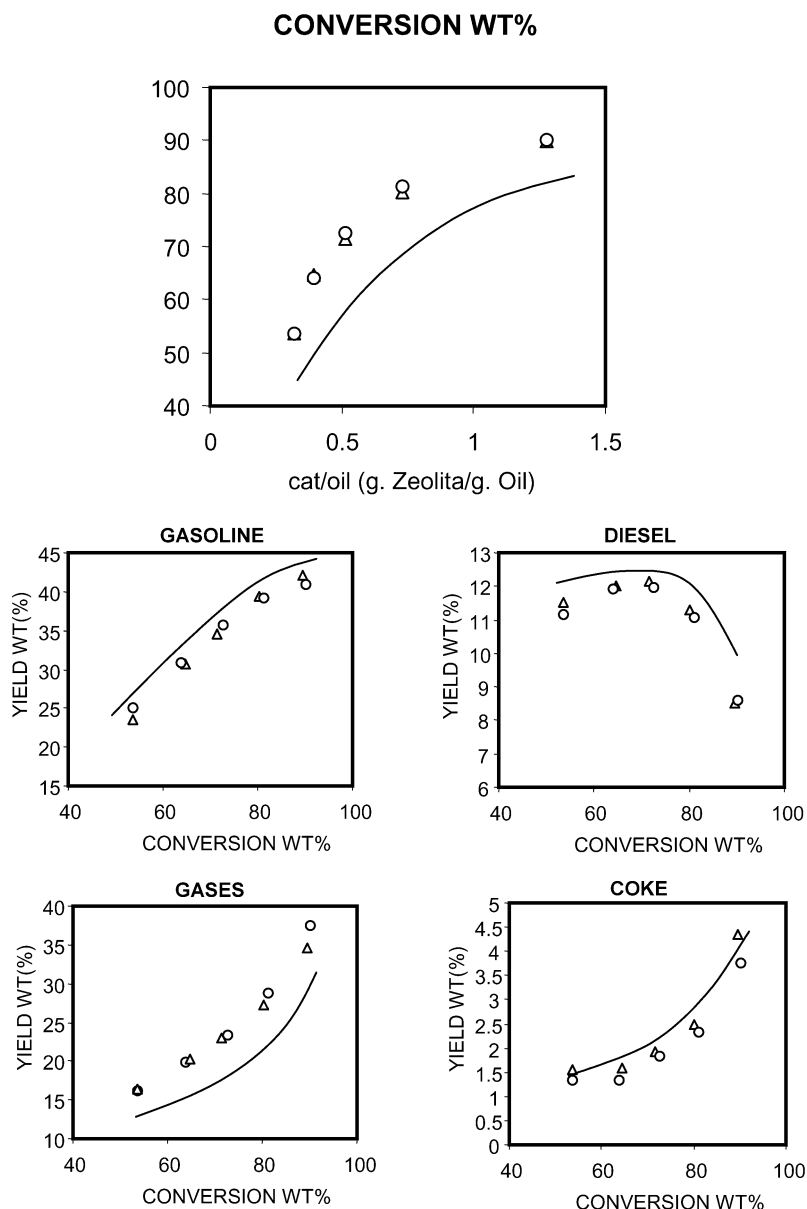


Fig. 6. Total conversion and selectivities in the cracking of gasoil at 793 K and 30 s time on stream over (line) USY as base catalyst and (○) ZSM-5 and (△) SiGeAl-ITQ-13 at 20 wt% of additive level.

of ITQ-13 and ZSM-5 appear to indicate that more EFAL is present in the former despite the fact that its starting framework Al content was lower. The same conclusion can be reached by looking into the pyridine associated with Lewis acid sites related to the presence of EFAL in the zeolite [39] (see Table 3). Indeed, Lewis acidity, as measured by pyridine coordinated to EFAL, is higher in the Al-ITQ-13 samples.

Nevertheless, it is worth mentioning that despite the presence of Ge in the SiGeAl-ITQ-13 sample, which decreases the average Sanderson electronegativity [40] and thus the acid strength, pyridine desorption results at different temperatures indicate that the proportion of the stronger acid sites is larger in the ITQ-13 sample (see Table 3). This is likely due to an electronic confinement effect in the narrower pores of ITQ-13 [41]. Moreover, if we calculate the turnover frequencies by dividing the first-order kinetic rate constant in *n*-decane cracking by the

concentration of Brønsted acid sites retaining pyridine at 423 K, then the values given in Table 4 show that the turnover of the directly synthesized Al-ITQ-13 is close to that of ZSM-5.

It is clear that the narrower pores, stronger acidity, and high turnover numbers of ITQ-13 justifies the study of this material as a shape-selective FCC additive for producing propylene. We have studied this material for this purpose by performing catalytic cracking of a vacuum gasoil (characteristics of the feed given in Table 5) with a cracking catalyst comprising 1.2 g of USY (unit cell size, 2.426 nm) and different percentages of ZSM-5 or the directly synthesized Al-ITQ-13.

The cracking results presented in Fig. 6 show that, as can be expected, the introduction of the ZSM-5 or Al-ITQ-13 zeolite additives produces a decrease in the yield of gasoline and an increase in the amount of gases. However, Al-ITQ-13 gives a significantly higher propylene-to-propane ratio in the gases than

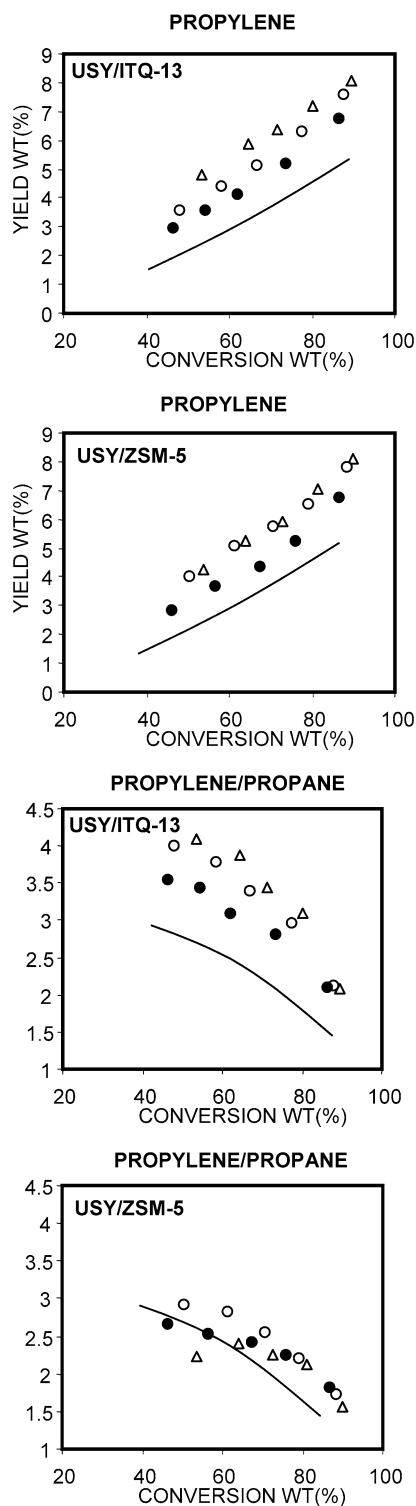


Fig. 7. Propylene yields and propylene/propane ratios in the cracking of gasoil at 793 K and 30 s time on stream over (line) USY as base catalyst and ZSM-5 or SiGeAl-ITQ-13 at (●) 5, (○) 10 and (△) 20 wt% of additive level.

ZSM-5 (see Fig. 7). Moreover, the sensitivity of the propylene-to-propane ratio to the amount of zeolite additive introduced is also higher for ITQ-13.

Because crystal size and shape differ between ZSM-5 and ITQ-13 (see Fig. 8 and Table 3), we have studied here the

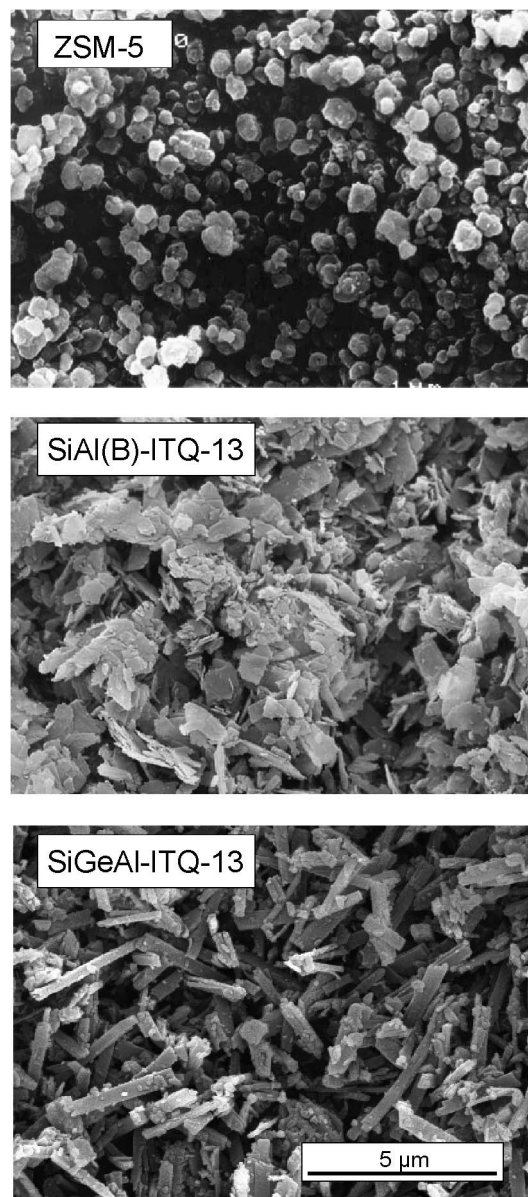


Fig. 8. Scanning electron microscopy of ZSM-5, SiAl(B)-ITQ-13 and SiGeAl-ITQ-13.

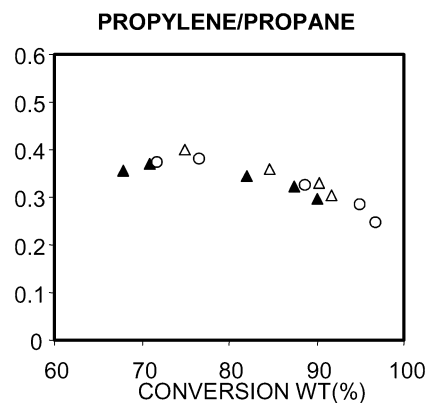


Fig. 9. Propylene/propane ratio in the cracking of *n*-decane at 773 K and 60 s time on stream over zeolites ZSM-5 (Si/Al = 15) of different crystal size: (△) 0.2, (○) 0.5, and (▲) 1 μm.

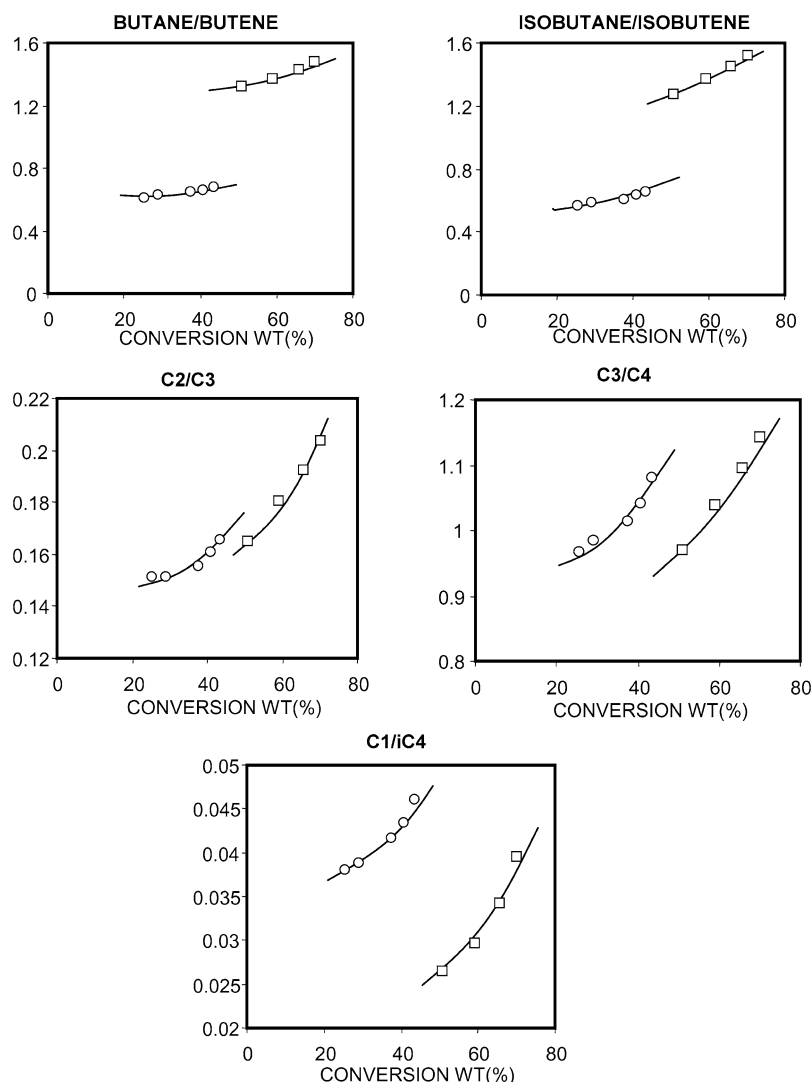


Fig. 10. Different hydrogen transfer and electric field gradient ratios in the cracking of *n*-decane at 773 K and 60 s time on stream over (□) ZSM-5 and (○) SiGeAl-ITQ-13.

effect of crystal size on the propylene-to-propane ratio. SiGeAl-ITQ-13 is formed by elongated crystals in which the sinusoidal 10 MR channel ($4.8 \times 5.7 \text{ \AA}$) occurs along the *c*-axis with a length of 0.5–3 μm (see Table 3), whereas the other 10 and the 9 MR channels are disposed perpendicularly along the *a*–*b* plane, the one with the smaller crystal dimension. So from the standpoint of reactivity, the pore length of the 9 MR channels should be considered to be 0.2–0.3 μm . To study the influence of crystallite size on the propylene-to-propane ratio, and to check whether selectivity differences between ZSM-5 and ITQ-13 can be due to the somewhat different length of the pores (different crystal sizes), we carried out the cracking of *n*-decane on three ZSM-5 samples with the same Si/Al ratio and average crystal sizes of 0.2, 0.5, and 1 μm . The catalytic results obtained (propylene-to-propane ratio) with these three samples (Fig. 9) confirm that in the range of 0.2–1 μm , we cannot see any influence on selectivity. Therefore, we can assume that differences in selectivity (propylene/propane) observed with ITQ-13 and ZSM-5 can be attributed not to differences in crystal size, but rather to other factors.

Thus the important improvement in the propylene-to-propane ratio achieved with Al-ITQ-13 can be due to the smaller pore dimensions of this zeolite as well as to the somewhat higher Si/Al ratio. Both factors increase the electric field gradient and decrease bimolecular hydrogen transfer reactions [42]. The influence of these two parameters has been tested by analyzing the C_1/iC_4 , C_2/C_3 , C_3/C_4 , iC_4/iC_4^- , and C_4/C_4^- ratios in the cracking of *n*-decane. The C_1/iC_4 , C_2/C_3 , and especially C_3/C_4 ratios should be larger with a larger electric field within the pores of the zeolites [42]. Meanwhile, the higher the iC_4/iC_4^- and C_4/C_4^- , the higher the ratio of hydrogen transfer to cracking [43,44]. Taking into account these findings, the results presented in Fig. 10 confirm that the electric field gradient is higher in Al-ITQ-13, whereas the hydrogen transfer/cracking ratio is higher in ZSM-5.

4. Conclusion

We have found that when introducing Ge in the synthesis of ITQ-13, it is possible to prepare Al-ITQ-13 directly by

synthesis, avoiding the boron form and ulterior ion exchange. This approach makes it possible to achieve lower framework T^{IV}/T^{III} ratios, and also to perform the synthesis in a fluoride-free medium. The directly synthesized Al-ITQ-13 with a lower T^{IV}/T^{III} ratio shows higher acidity and catalytic activity for *n*-decane cracking than the Al-ITQ-13 prepared by the indirect route.

Compared with ZSM-5, Al-ITQ-13 has a lower number of acid sites due to its higher Si/Al ratio and a more extensive dealumination occurring during calcination; however, the acid strength shown by the pyridine adsorption is higher in ITQ-13. The stronger field gradients present in ITQ-13 and the smaller pore dimensions improve the shape-selectivity for cracking linear olefins in the gasoline range, increasing the propylene/propane ratio with respect to ZSM-5.

Acknowledgment

The authors thank the CICYT (MAT 2003-07945-C02-01) for financial support.

References

- [1] C.S. Cundy, P.A. Cox, *Microporous Mesoporous Mater.* 82 (2005) 1.
- [2] C.S. Cundy, P.A. Cox, *Chem. Rev.* 103 (2003) 663.
- [3] S.I. Zones, *Stud. Surf. Sci. Catal.* 158 (2005) 1.
- [4] A. Burton, S. Elomari, C.Y. Chen, R.C. Medrud, I.Y. Chan, L.M. Bull, C. Kibby, T.V. Harris, S.I. Zones, E.S. Vittoratos, *Chem.-Eur. J.* 9 (2003) 5737.
- [5] K.G. Strohmaier, D.E.W. Vaughan, *J. Am. Chem. Soc.* 125 (2003) 16035.
- [6] A. Corma, M.J. Diaz-Cabañas, F. Rey, S. Nicolopoulos, K. Boulahya, *Chem. Commun.* (2004) 1356.
- [7] J.L. Paillaud, B. Harbuzaru, J. Patarin, N. Bats, *Science* 304 (2004) 990.
- [8] A. Burton, S. Elomari, R.C. Medrud, I.Y. Chan, C.Y. Chen, L.M. Bull, E.S. Vittoratos, *J. Am. Chem. Soc.* 125 (2003) 1633.
- [9] A. Corma, M.J. Diaz-Cabañas, J. Martinez-Triguero, F. Rey, J. Rius, *Nature* 418 (2002) 514.
- [10] A. Cantin, A. Corma, S. Leiva, F. Rey, J. Rius, S. Valencia, *J. Am. Chem. Soc.* 127 (2005) 11560.
- [11] S. Ernst, S.P. Elangovan, M. Gerstner, M. Hartmann, T. Hecht, S. Sauerbeck, *Stud. Surf. Sci. Catal.* 154 (2004) 2861.
- [12] R. Castañeda, A. Corma, V. Fornes, F. Rey, J. Rius, *J. Am. Chem. Soc.* 125 (2003) 7820.
- [13] A. Corma, F. Rey, J. Rius, M.J. Sabater, S. Valencia, *Nature* 431 (2004) 287.
- [14] A. Burton, S. Elomari, *Chem. Commun.* (2004) 2618.
- [15] G.S. Lee, S.I. Zones, *J. Solid State Chem.* 167 (2002) 289.
- [16] M.G.G. Wu, M.W. Deem, S.A. Elomari, R.C. Medrud, S.I. Zones, T. Maesen, C. Kibby, C.Y. Chen, I.Y. Chan, *J. Phys. Chem. B* 106 (2002) 264.
- [17] D.L. Dorset, G.J. Kennedy, *J. Phys. Chem. B* 108 (2004) 15216.
- [18] Y.X. Wang, H. Gies, B. Marler, U. Muller, *Chem. Mater.* 17 (2005) 43.
- [19] P.A. Vaughan, *Acta Crystallogr.* 21 (1966) 983.
- [20] G.T. Kokotailo, J.L. Schlenker, F.G. Dwyer, E.W. Valyocsik, *Zeolites* 5 (1985) 349.
- [21] S.A.I. Barri, G.W. Smith, D. White, D. Young, *Nature* 312 (1984) 533.
- [22] P. Wagner, S.I. Zones, M.E. Davis, R.C. Medrud, *Angew. Chem. Int. Ed.* 38 (1999) 1269.
- [23] G.T. Kokotailo, S.L. Lawton, D.H. Olson, D.H. Olson, W.M. Meier, *Nature* 272 (1978) 437.
- [24] A. Corma, *J. Catal.* 216 (2003) 298.
- [25] G. Bellussi, P. Pollesel, *Stud. Surf. Sci. Catal.* 158 (2005) 1202.
- [26] A. Corma, V. Gonzalez-Alfaro, A.V. Orchilles, *Appl. Catal. A* 187 (1999) 245.
- [27] A. Corma, A.V. Orchilles, *Microporous Mesoporous Mater.* 35 (2000) 21.
- [28] T. Boix, M. Puche, M. Cambor, A. Corma, *US Patent* 6 471 941 (2002).
- [29] A. Corma, M. Puche, F. Rey, G. Sankar, S.J. Teat, *Angew. Chem., Int. Ed.* 42 (2003) 1156.
- [30] A. Corma, *US Patent* 6 709 572 (2003).
- [31] C.A. Emeis, *J. Catal.* 141 (1993) 347.
- [32] A. Corma, J. Martinez-Triguero, C. Martinez, *J. Catal.* 197 (2001) 151.
- [33] T. Blasco, A. Corma, M.J. Diaz-Cabañas, F. Rey, J.A. Vidal-Moya, C.M. Zicovich-Wilson, *J. Phys. Chem. B* 106 (2002) 2634.
- [34] T. Blasco, A. Corma, M.J. Diaz-Cabañas, F. Rey, J. Rius, G. Sastre, J.A. Vidal-Moya, *J. Am. Chem. Soc.* 126 (2004) 13414.
- [35] A. Corma, M.T. Navarro, F. Rey, J. Rius, S. Valencia, *Angew. Chem. Int. Ed.* 40 (2001) 2277.
- [36] J.L. Guth, H. Kessler, P. Caullet, J. Hazm, A. Merrouche, in: R. Von Ballmoos, J.B. Higgins, M.J.M. Treacy (Eds.), *Proc. 9th. Intl. Zeolite Conf., Butterworth-Heinemann, Montreal, 1993*, p. 215.
- [37] R.F. Lobo, M.E. Davis, *Microporous Mater.* 3 (1994) 61.
- [38] G. Engelhard, D. Michel, *High Resolution Solid-State NMR of Silicates and Zeolites*, Wiley, New York, 1987.
- [39] J.W. Ward, *J. Catal.* 9 (1967) 225.
- [40] W.J. Mortier, *J. Catal.* 55 (1978) 138.
- [41] F. Marquez, H. Garcia, E. Palomares, L. Fernandez, A. Corma, *J. Am. Chem. Soc.* 122 (2000) 6520.
- [42] C. Mirodatos, D. Barthomeuf, *J. Catal.* 114 (1988) 121.
- [43] E. Benazzi, T. Chapus, T. Cheron, H. Cauffriez, C. Marcilly, *Stud. Surf. Sci. Catal.* 84 (1994) 1663.
- [44] S. Jolly, J. Saussey, M.M. Bettahar, J.C. Lavalley, E. Benazzi, *Appl. Catal. A* 156 (1997) 71.